NASA TECHNICAL NOTE

NASA TN D-6162

NASA TN D-6162

SOME CHARACTERISTICS OF A BOILING-WATER-COOLED VAPOR TRANSPORT FUEL PIN

by James R. McConaghy, Jr.

Lewis Research Center
Cleveland, Ohio 44135

NATIONAL AERONAUTICS AND SPACE ADMINISTRATION • WASHINGTON, D. C. • FEBRUARY 1971

1. Report No.	2. Government Accession No.	3. Recipient's Catalog No.
NASA TN D-6162		

4. Title and Subtitle	5. Report Date
SOME CHARACTERISTICS OF A BOILING-WATER-COOLED VAPOR TRANSPORT FUEL PIN	February 1971
	6. Performing Organization Code
7. Author(s)	8. Performing Organization Report No.
James R. McConaghy, Jr.	E-5675
	10. Work Unit No.
9. Performing Organization Name and Address	122-28
Lewis Research Center National Aeronautics and Space Administration Cleveland, Ohio 44135	11. Contract or Grant No.
	13. Type of Report and Period Covered
12. Sponsoring Agency Name and Address	Technical Note
National Aeronautics and Space Administration Washington, D. C. 20546	14. Sponsoring Agency Code

15. Supplementary Notes

16. Abstract

The behavior of a boiling-water-cooled vapor transport fuel pin is studied with the aid of a computer code. Pin behavior is investigated at high power output in the region of the boiling burnout point. A comparison is made that shows that much higher power densities can be obtained from a vapor transport fuel pin than from a conventional solid fuel pin design at pin diameters above 1 centimeter.

17. Key Words (Suggested by Author(s))	18. Distribution Statement
Fuel element Reactor Burn-up Vapor-transport	Unclassified - unlimited

19. Security Classif. (of this report)	20. Security Classif. (of this page)	21. No. of Pages	22. Price*
Unclassified	Unclassified	28	$3.00

*For sale by the National Technical Information Service, Springfield, Virginia 22151

SOME CHARACTERISTICS OF A BOILING-WATER-COOLED VAPOR TRANSPORT FUEL PIN

by James R. McConaghy, Jr.

Lewis Research Center

SUMMARY

In this report the behavior of a boiling-water-cooled vapor transport fuel pin is investigated. This type of pin is provided with a central void that permits fuel material to move from regions of high heat generation (and temperature) to regions of lower heat generation. This characteristic tends to remove hot spots and can be exploited to some advantage. A heat-transfer analysis is used to study pin characteristics at startup and during steady-state operation. A comparison with a conventional solid fuel pin of similar design is made.

The study investigates the fuel pin in the region of boiling burnout heat flux. Fuel pin and coolant channel dimensions are fixed.

A comparison is made between vapor transport pins and conventional solid pins. For the particular case studied the average power density attainable in a vapor transport pin was 260 percent greater than in a conventional solid fuel pin.

It is shown that under certain conditions a vapor transport fuel pin can be operated in the film boiling heat-transfer regime without the clad material reaching failure temperatures. This suggests that it may be possible to produce superheated steam from a properly designed single stage reactor core.

INTRODUCTION

The use of vapor transport fuel pins has been suggested (ref. 1) as a means of extending the operating life of high power reactors. The vapor transport fuel pin is essentially a small pressure vessel with the fuel deposited on the inside surface. There is a relatively large central void.

The pin is designed to operate such that the inside surface of the fuel is at a high enough temperature to permit vapor phase mass transfer of the fuel within the void. The

movement of fuel within the void space tends to keep the inside fuel surface temperature constant and thus eliminate hot spots. In addition, the void space provides a storage volume for the gaseous fission products, thereby minimizing the rate of fission gas pressure buildup. A more detailed description of the vapor transport fuel-pin concept is available in reference 1. The major conclusions reached in reference 1 were that a vapor transport type of fuel pin would have longer life and produce higher fuel burnup than a conventional fuel pin under similar operating conditions.

This report investigates the behavior of a single vapor transport fuel pin in a boiling-water-cooled reactor. Boiling-water reactors are of considerable practical interest because of their relative simplicity and because of the high pin surface heat fluxes attainable. In addition, boiling-water-cooled reactors are, at least to a degree, self-controlling (ref. 2). The design of an entire reactor system is not discussed here.

Two computer codes are used to simulate operation of the fuel pin. The first code simulates pin startup with an initial uniform fuel distribution (this analysis is also used for the solid pin calculations). The second code calculates pin characteristics at the final steady-state operating conditions after the fuel has redistributed to produce a uniform internal fuel surface temperature. Figure 1 illustrates the initial and steady-state fuel distributions. Only radial heat conduction is considered within the pin. External heat transfer is to a flowing boiling-water coolant stream.

This report presents a study of a 2.03-centimeter (0.800-in.) outside-diameter vapor transport fuel pin that is 122 centimeters (4 ft) long. The operation of this pin is studied through the region of the critical heat flux. Critical heat flux is defined herein as the point at which departure from nucleate boiling or "burnout" occurs.

The vapor transport fuel pin is compared with a solid fuel pin under similar operating conditions. The power distribution and power densities of the two types of pins are compared and discussed.

This report does not fully investigate the behavior of the vapor transport fuel pin under all conditions. The main purpose here is to consider one particular case in order to illustrate some of the characteristics and advantages of designing a fuel pin to operate as a vapor transport pin. Emphasis is placed on the heat-transfer aspects of the pin's operation. An analysis of the fuel pin lifetime as a function of deisgn parameters is available in a previous report by Rom, Finnegan, and McDonald (ref. 1).

SYMBOLS

A_c cross sectional area of coolant annulus

C_P heat capacity of coolant

C_{P_S} heat capacity of coolant at fuel-pin surface temperature

C_{PV} heat capacity of vapor phase coolant

C_2 heat generated per unit thickness of fuel per thermal neutron

C_3 thermal neutron attenuation coefficient

C_4 temperature dependency coefficient of liquid phase coolant density

c constant of integration

d_{eq} equivalent hydraulic diameter of coolant annulus

e fuel enrichment

h_1 liquid phase convective heat-transfer coefficient

h_4 vapor phase convective heat-transfer coefficient

J index used to identify axial increment in fuel-pin heat-transfer calculation

k_2 thermal conductivity of fuel

k_3 thermal conductivity of clad

k_4 thermal conductivity of bulk coolant

$k_{4,s}$ thermal conductivity of coolant at fuel-pin surface temperature

L fueled length of fuel pin

N total number of axial increments used in fuel-pin calculations

$P_{(J)}$ power produced in axial increment Δz of fuel pin

P_c coolant system pressure

Q_w heat generation rate per unit volume of fuel at the exterior fuel surface

Q_2 heat generation rate per unit volume of fuel

q_{f-c} heat flux at the fuel-clad interface

q_{LB} local boiling heat flux

q_i fully developed nucleate boiling heat flux at the value of $T_s - T_{sat}$ at which local boiling first occurs

q_o heat flux at the fuel-pin surface

R_a radius of coolant annulus

R_i radius of central void

R_o outside radius of fuel-pin clad

R_w inside radius of fuel-pin clad

r distance from fuel-pin centerline

T_i temperature of internal fuel surface

T_s temperature of external clad surface

T_{sat} saturation temperature of coolant

T_w temperature of internal clad surface

T_2 fuel temperature

T_3 clad temperature

T_4 bulk coolant temperature

V linear velocity of coolant

z distance from coolant inlet end of fuel pin

Δz length of one axial increment used in heat-transfer calculation

α volume fraction of vapor in coolant

ϵ effective emissivity

λ latent heat of vaporization of coolant

μ viscosity of coolant

μ_s viscosity of coolant at fuel-pin surface temperature

ρ density of coolant

ρ_f density of fuel

ρ_L density of liquid coolant at saturation

ρ_s density of coolant at fuel-pin surface temperature

ρ_v density of vaporized coolant at saturation

σ Stefan-Boltzman constant

ϕ thermal neutron flux at fuel-clad interface

ϕ_o unperturbed peak thermal neutron flux at fuel-clad interface

χ mass fraction of vapor in coolant

Superscripts:

(1) convective heat-transfer regime

(2) transition region from convective heat transfer to fully developed nucleate boiling

(3) fully developed nucleate boiling regime

(4) film boiling regime

— indicates an arithmetic average

ANALYSIS

The mathematical analysis of the fuel pin is developed in two parts. First, the fuel distribution is assumed to have uniform thickness for the entire pin length. Using this initial fuel distribution, a known axial neutron flux profile and known coolant inlet conditions, temperature and power profiles, are calculated. The first case predicts the maximum temperature and power level at system startup.

The second case determines the required fuel load and fuel distribution necessary to produce a desired constant internal fuel surface temperature as a function of the peak heat flux. The program also has an option that will compute the internal temperature corresponding to a specified fuel load after fuel redistribution. The temperature and power distributions are then determined for this final operating condition of the pin which would exist after fuel redistribution.

Both cases are steady-state solutions; one is the initial condition, and the other is the final condition.

General Development of the Heat Conduction Equations

The analysis is formulated with the following restrictions and assumptions:

(1) End effects are negligible.

(2) Fuel distribution and pin geometry are axisymmetric.

(3) Heat conduction in the axial direction is negligible.

(4) An average radial thermal conductivity for each material or region that is representative of the true temperature-dependent situation is used. This radial-average thermal conductivity is recalculated for each axial location.

(5) The internal void space temperature at any given axial position is constant and equal to the internal fuel surface temperature, T_i, at that position.

A schematic diagram of the pin model is given in figure 2.

Based on restrictions (1) to (5) the heat transfer in the fuel shell is considered first.

For a thermal conductivity that is constant in the radial direction at any given axial location and for conduction in the radial direction only, the heat conduction equation is,

$$\frac{d\left[r \frac{dT_2(r)}{dr}\right]}{dr} = \frac{-rQ_2(r)}{k_2} \tag{1}$$

With the boundary condition

$$r\left[\frac{dT_2(r)}{dr}\right]_{r=R_i} = 0 \tag{2}$$

integration gives

$$\frac{dT_2(r)}{dr} = \frac{-1}{rk_2}\int_{R_i}^{r} rQ_2(r)dr \tag{3}$$

Integrating again from $r = R_i$ to $r = R_w$ results is

$$T_w = T_i - \frac{1}{k_2}\int_{R_i}^{R_w}\frac{1}{r}\int_{R_i}^{r} rQ_2(r)drdr \tag{4}$$

where T_w is the temperature at the fuel-clad interface.

The heat conduction equation that describes the heat flow through the clad is

$$\frac{d\left[r\,\frac{dT_3(r)}{dr}\right]}{dr} = 0 \tag{5}$$

Integrating once results in

$$r\,\frac{dT_3(r)}{dr} = c \tag{6}$$

where c is a constant.

The heat flux at the fuel-clad interface q_{f-c} is

$$q_{f-c} = -k_3\,\frac{dT_3(r)}{dr}\bigg|_{R_w} = -k_2\,\frac{dT_2(r)}{dr}\bigg|_{R_w} \tag{7}$$

Therefore,

$$c = \frac{-R_w q_{f-c}}{k_3} \tag{8}$$

and

$$\frac{dT_3(r)}{dr} = \frac{-R_w q_{f-c}}{r k_3} \tag{9}$$

Integrating from $r = R_w$ to $r = R_o$ yields

$$T_s = T_w - \frac{R_w q_{f-c}}{k_3} \ln\left(\frac{R_o}{R_w}\right) \tag{10}$$

The heat flux at the fuel-clad interface q_{f-c} is simply the power generated in a length (increment) of fuel Δz divided by the interfacial area or

$$q_{f-c} = \frac{P_{(J)}}{2\pi R_w \Delta z} \tag{11}$$

if power is constant over Δz. The power generation is given by

$$P(J) = 2\pi \Delta z \int_{R_i}^{R_w} r Q_2(r) dr \tag{12}$$

Equations (4) and (10) to (12) completely describe the radial heat transfer in the pin.

A computer code used to calculate the characteristics of the pin at startup is described in the next section.

Case 1: Description of Computer Code Used for Startup Calculations

The fuel pin is broken up into N axial increments such that the values of the axial (z) coordinate index J run from $J = 1$ at $z = 0$ to $J = N$ at $z = L$ (see fig. 2). The value of z associated with the J^{th} increment is the midpoint of that increment. The $J = 1$ and $J = N$ increments have a length of $\frac{1}{2} \Delta z$. The value of N is chosen such that increasing the value has little effect (within ±1 percent) on the calculated pin operation.

The heat generation $Q_2(r)$ is a function of the thermal neutron flux $\phi(z)$. The flux profile is assumed to be a truncated sinusoid modified by the volume fraction of vapor α in the coolant channel such that

$$\left(\frac{e}{0.93}\right) \phi(z) = \phi_o \left(1 - \frac{\alpha}{2}\right) \sin\left[0.201 + 0.870\pi \left(\frac{z}{L}\right)\right] \tag{13}$$

where ϕ_o is the peak flux that would reach the fuel if there were no voids in the coolant channel and where e is the enrichment. Equation (13) is assumed to be representative of a typical axial flux profile in a boiling water reactor.

The heat generation rate at the fuel-clad interface $Q_w(z)$ is taken as

$$Q_w(z) = C_2\phi(z) \tag{14}$$

where C_2 is a function of the fuel type. For the purpose of this report the heat-generation rate is assumed to vary with radial position as

$$Q_2(r,z) = Q_w(z)e^{-C_3(R_w-r)} \tag{15}$$

where C_3 is a thermal neutron flux attenuation coefficient. The use of a slab geometry equation simplifies integration and is valid for the thin fuel shell typical of a vapor transport fuel pin.

The power generated by any fuel segment of length Δz is then

$$P = 2\pi\Delta z\, Q_w(z) \int_{R_i}^{R_w} r\, e^{-C_3(R_w-r)}\, dr \tag{16}$$

This particular expression may be integrated analytically. The computer code is set up to evaluate the integral numerically so that any form of a power integral may be used.

The pin is assumed to be surrounded by coolant in a channel of annular cross sectional area A_c. The coolant properties are calculated on the basis of energy added to the coolant in the $(J-1)^{th}$ increment. If

$$T_{4(J-1)} < T_{sat} \tag{17}$$

then the coolant is subcooled and

$$T_{4(J)} = T_{4(J-1)} + \frac{P_{(J-1)}}{V_{(J-1)}A_c\,\rho_{(J-1)}C_P} \tag{18}$$

$$\rho_{(J)} = C_4\,\rho_{(J-1)} \tag{19}$$

$$V_{(J)} = \frac{V_{(J-1)}\,\rho_{(J-1)}}{\rho_{(J)}} \tag{20}$$

If

$$T_{4(J-1)} \geq T_{sat} \tag{21}$$

and

$$\sum_{J=1}^{J} P_{(J)} \leq A_c V_{(1)} \rho_{(1)} \left[C_P \left(T_{sat} - T_{4(1)} \right) + \lambda \right] \tag{22}$$

then the coolant is at the saturation temperature and $T_{4(J)}$ is set equal to T_{sat}. The coolant density and velocity are then given by

$$P_{(J)} = \frac{V_{(J-1)} \rho_{(J-1)}}{\left[\left(\frac{P_{(J-1)}}{\lambda A_c} \right) \left(\frac{1}{\rho_V} - \frac{1}{\rho_L} \right) + V_{(J-1)} \right]} \tag{23}$$

$$V_{(J)} = \frac{V_{(J-1)} \rho_{(J-1)}}{\rho_{(J)}} \tag{24}$$

If

$$\sum_{J=1}^{J} P_{(J)} > A_c V_{(1)} \rho_{(1)} \left[C_P \left(T_{sat} - T_{4(1)} \right) + \lambda \right] \tag{25}$$

then the coolant is superheated and

$$T_{4(J)} = \frac{\left\{ -A_c V_{(1)} \rho_{(1)} \left[C_P \left(T_{sat} - T_{4(1)} \right) + \lambda \right] + \sum_{J=1}^{J} P_{(J)} + A_c V_{(1)} \rho_{(1)} C_{P_V} T_{sat} \right\}}{A_c V_{(1)} \rho_{(1)} C_{P_V}} \tag{26}$$

$$\rho_{(J)} = \rho_{(J-1)} \left(\frac{T_{4(J-1)}}{T_{4(J)}} \right) \tag{27}$$

and $V_{(J)}$ is calculated as in equation (24) where $T_{(J)}$ and $T_{(J-1)}$ must be absolute temperatures.

The steam quality on a mass basis in the coolant channel at increment J is

$$x = \left(\frac{\frac{\rho_L}{\rho_{(J)}} - 1}{\frac{\rho_L}{\rho_V} - 1} \right) \tag{28}$$

The void fraction of steam on a volume basis is

$$\alpha = \frac{\rho_{(J)} - \rho_L}{\rho_V - \rho_L} \tag{29}$$

Except for the first increment where $T_{i(1)}$ is read in, $T_{i(J)}$ is first assumed to be equal to $T_{i(J-1)}$. Then using equation (4)

$$T_w = T_i - \frac{1}{k_2} \int_{R_i}^{R_w} \frac{1}{r} \int_{R_i}^{r} r Q_2(r) dr dr \tag{4}$$

the temperature at the fuel-clad interface T_w can be calculated. Then

$$T_s = T_w - \frac{R_w q_{f-c}}{k_3} \ln\left(\frac{R_o}{R_w}\right) \tag{10}$$

is used to calculate the fuel-pin surface temperature T_s.

By using the calculated surface temperature and the calculated coolant temperature and physical properties (eqs. (17) to (29)), a heat-transfer rate to the coolant may be determined.

This value is compared with the rate necessary to dissipate the energy generated by fission. If the two heat fluxes do not match within ±0.1 percent, a new value of $T_{i(J)}$ is assumed, and $T_{s(J)}$ is recalculated. When the heat fluxes match within ±0.1 percent, the code continues to the $(J+1)^{th}$ increment.

Appropriate subroutines are used to calculate the heat-transfer rate to the coolant and to calculate temperature dependent physical properties. These are discussed in appendixes A and B.

The code is written to accept all data in SI units except pressure, which is expressed in atmospheres absolute, and temperature, which is in ^{o}C.

Case 2: Description of the Computer Code Used for the Fully Redistributed Fuel Calculations

The indexing of the axial increments of the fuel pin is done in the same manner as for the startup calculation (case 1).

The thermal neutron flux distribution, heat generation rate, and power output are calculated as they were in the startup code. The appropriate relations are

$$\left(\frac{e}{0.93}\right)\phi(z) = \phi_o\left(1 - \frac{\alpha}{2}\right)\sin\left[0.201 + 0.870\pi\left(\frac{z}{L}\right)\right] \tag{13}$$

$$Q_w(z) = C_2\phi(z) \tag{14}$$

$$Q_2(r,z) = Q_w(z)e^{-C_3(R_w-r)} \tag{15}$$

$$P_{(J)} = 2\pi\Delta z\, Q_w(z)\int_{R_i}^{R_w} r\, e^{-C_3(R_w-r)}\,dr \tag{16}$$

Again, the pin is assumed to be surrounded by coolant in a channel of annular cross sectional area A_c. The coolant properties are calculated on the basis of energy added to the coolant in the $(J-1)^{th}$ increment. The method of calculation is shown in equations (17) to (29) in the previous section.

This code is written to operate in two different modes. Mode one calculates the fuel loading necessary to produce a preselected void temperature. Mode two calculates the internal void temperature obtained from a preselected fuel loading.

Mode one was used for most of the calculations in this report and is the basis for the following discussion.

An internal temperature T_i is input. This temperature should be high enough to permit a reasonable rate of vapor transport in the void space (2600^{o} C for UO_2 fuel is used in this report).

Except for the first increment where $R_{i(1)}$ is read in, $R_{i(J)}$ is first assumed to be equal to $R_{i(J-1)}$. Then using equation (16),

$$P_{(J)} = 2\pi\Delta z\, Q_{w(J)} \int_{R_i}^{R_w} r\, e^{-C_3(R_w - r)}\, dr \tag{16}$$

the power generated in the J^{th} increment is calculated. The heat flux that must be transferred from the pin surface is then

$$q_{o(J)} = \frac{P_{(J)}}{2\pi\Delta z R_o} \tag{30}$$

The heat-transfer subroutine is then called (see appendix A) and the surface temperature necessary to obtain a heat flux of $q_{o(J)}$ is calculated.

The temperature of the inside surface of the fuel clad T_w can then be obtained by substituting $q_{f-c} = q_o \left(\frac{R_o}{R_w}\right)$ into equation (10),

$$T_w = T_s - \frac{R_o q_o}{k_3} \ln\left(\frac{R_w}{R_o}\right) \tag{31}$$

By rearranging equation (4) the internal temperature T_i can then be obtained

$$T_i = T_w + \frac{1}{k_2} \int_{R_{i(J)}}^{R_w} \frac{1}{r} \int_{R_{i(J)}}^{r} r Q_{w(J)} e^{-C_3(R_w - r)}\, dr\, dr \tag{32}$$

If this internal temperature does not agree to within ±0.1 percent with the desired temperature, a new value of $R_{i(J)}$ is selected and $T_{i(J)}$ is reculated. When the calculated and desired internal temperatures compare within ±0.1 percent, the code continues to the $(J+1)^{th}$ increment.

The fuel mass in each increment is calculated and summed to give the total mass of fuel necessary to produce the selected internal temperature.

If the operation is in mode two, then the calculated fuel mass is compared with the desired fuel mass. If they do not compare within ±0.1 percent a new value of the desired internal temperature is selected, and the entire mode one process is repeated.

The temperature dependent physical property subroutine is discussed in appendix B.

Again the code is written to accept all data in SI units except pressure, which is in atmospheres absolute, and temperature which is in ^{o}C.

DISCUSSION

A study of a vapor transport fuel pin has been done using the computer codes described in the analysis section. The simplifying assumptions made in the development of the mathematical model should result in conservative calculations of pin behavior. Although refinements in the model could be made, the approach used here should not result in any gross errors.

Curves are presented to illustrate the major characteristics of the vapor transport pin. A comparison between a vapor transport pin and a similar solid-fuel pin is made and the implications discussed.

General Description of the System

The study presented in this report is based on a 122-centimeter (4-ft) long, 2.03-centimeter (0.8-in.) outside-diameter pin. The clad is 0.254-centimeter (0.1-in.) thick AISI 347 stainless steel. The fuel is uranium dioxide.

The coolant is water at a pressure of 6.9×10^6 newtons per square meter (68 atm) in an annular channel. The pin is in a vertical position with upward coolant flow.

The unperturbed neutron flux at the fuel-clad interface is assumed to be a chopped sinusoid (axially) and symmetric in the angular direction. The actual flux at the fuel-clad interface is a function of the void fraction of steam in the coolant channel, as described by equation (13). In this equation, the flux is assumed to be proportional to the mass of water in the surrounding coolant flow channel. This model is intended to give an axial flux variation that is somewhat representative of the actual variation that would exist in a boiling water reactor. For any particular reactor, the actual axial flux variation should be used in the code.

A reference case was selected as a basis for the calculations. The values of the major parameters for this case are as follows:

Pin length, L, cm	122.0
Outside clad radius, R_o, cm	1.015
Inside clad radius, R_w, cm	0.762
Radius of coolant annulus, R_a, cm	1.602
Coolant pressure, P_c, N/m^2	6.895×10^6
Coolant velocity, V, cm/sec	305.0
Coolant inlet temperature, T_4, ^oC	275.0
Unperturbed peak neutron flux, $\phi_o(0.93/e)$, neutron/cm^2sec	1.6×10^{13}
Internal fuel surface temperature, T_L, ^oC	2600.0

The values of the constants used in the calculations are as follows:

Heat generation rate per thermal neutron, C_2, cal/cm-m	1.0174×10^{-10}
Neutron flux attenuation coefficient, C_3, cm^{-1}	4.05
Density variation coefficient of liquid phase coolant, C_4, dimensionless	1.0
Number of axial increments in computer calculation, N, dimensionless	100
Density of fuel, ρ_f, g/cm^3	10.96

Effect of Neutron Flux

The unperturbed peak neutron flux $\phi_o(0.93/e)$ where e is the enrichment, is used as input data to the code as a means of changing the heat generation rate per unit volume of fuel. Figure 3 is a plot of the peak internal and external clad temperatures as a function of $\phi_o(0.93/e)$. The calculation is for the reference case with fuel redistribution and a fuel loading sufficient to produce a constant internal fuel surface temperature of 2600^o C. The sharp discontinuity in the curves between $\phi_o(0.93/e) = 1.7 \times 10^{13}$ and $\phi_o(0.93/e) = 1.8 \times 10^{13}$ neutrons per square centimeter per second indicates a transition of the coolant from fully developed nucleate boiling to film boiling ("boiling burnout point"). As neutron flux level increases, fuel loading must decrease to maintain constant fuel internal surface temperature (2600^o C). However, the heat flux increases until film boiling burnout occurs.

Initial Conditions

Calculations were made to determine the initial temperature distribution for a fuel pin loaded with 1500 grams of uranium dioxide (the fuel load of the reference case), uniformly distributed on the pin walls as shown in figure 1. The pin was assumed to be exposed to the same neutron flux level as the reference case ($\phi_o(0.93/e) = 1.6 \times 10^{13}$ neutrons/(cm^2)(sec) unperturbed peak flux). The resulting internal temperature profile is plotted in figure 4. The temperature spike at the center of the pin is due to film boiling of the coolant. Obviously the temperatures calculated would never be reached in reality because of redistribution of the fuel due to vapor transport. However, several important conclusions can be drawn from this initial-condition calculation.

(1) If the fuel is not shaped initially to approximate the steady-state operating fuel profile, attention must be given to startup rates.

(2) Internal temperatures high enough to cause vapor transport of the fuel ($\sim 2600^o$ C) can be reached before boiling burnout conditions are reached at the pin outer surface.

(3) The method of calculation presented here should be extended to investigate the transient behavior of the fuel pin.

Production of Superheated Steam

The present analysis indicates that it is possible to design a system to produce superheated steam. One particular case is illustrated in figure 5. The data for this calculation are identical to the data for the reference case of the parametric study, with the exception of the coolant annulus radius which is reduced from 1.602 to 1.300 centimeters. The reduced mass flow rate of coolant results in a higher void fraction of steam being generated. This flattens the neutron flux profile. Film boiling, due to the high steam void fraction, occurs at all flux levels in figure 5.

By operating a reactor in this manner it may be possible to produce superheated steam in a single-stage system without exceeding clad temperature limitations.

Comparison of the Vapor Transport Pin With a Similar Conventional Pin

The power density produced by a conventional fuel pin almost completely filled with fuel (0.02 mm central void) was compared with that of a similar pin operating as a vapor transport type of pin. Two constraints were put on the operation of the pins: (1) the centerline temperature must remain at or below 2600^{o} C, and (2) the critical heat flux must not be exceeded. The neutron flux level is a dependent variable in this calculation. It assumes whatever values are required by one of the two preceding constraints. In practice, the first constraint limits the operation of the conventional pin, and the second constraint limits the operation of the vapor transport pin.

The power density based on total pin volume attainable by both types of pins is plotted against outside pin diameter (constant clad thickness) in figure 6. The vapor transport pin permits much higher power densities than the conventional pin at pin diameters above 1.015 centimeters (0.4 in.). In the example, both pins are filled with fuel below a diameter of 1.015 centimeter (0.4 in.), and the curves coincide. The power density drops off only slightly with increasing diameter for the vapor transport pin. This suggests that if vapor transport pins were used, fewer pins of larger diameter could be used to construct a reactor without a major penalty in power density loss. The resulting economic benefit could be significant.

The higher power output of the vapor transport fuel pin is a result of two mechanisms. One, the internal fuel surface temperature of the vapor transport fuel pin is kept at 2600^{o} C for most of the pin length. Also, the fuel layer is much thinner than in the

conventional type pin. Therefore, because the insulating effect of the fuel is reduced, a higher surface heat flux without melting of the fuel is possible. Two, the heat flux profile for the vapor transport fuel pin is flatter in relation to the neutron flux profile than the heat flux profile for the conventional pin (fig. 7).

The vapor transport pin was shown in reference 1 to have other advantages. The central void of a vapor transport pin would extend the pin life significantly by slowing down the rate of pressure buildup due to the averaging out of the fission product gas accumulation. Also, the vapor transport of fuel would permit higher burnup fractions than possible in the conventional pin because of favorable replenishment of fuel from low reactivity worth zones to high reactivity worth zones. The dimensions and fuel loading of the example pins discussed in this report have not been optimized with respect of pin lifetime.

CONCLUSIONS

The performance of a vapor transport type of fuel pin in a boiling-water-cooled reactor has been studied using two computer codes. One code calculates pin startup (initial) conditions with uniform fuel distribution. The other code calculates final pin conditions at steady state with the fuel redistributed to produce an isothermal (constant) internal fuel surface temperature.

The fuel pin analyzed in this report is 122 centimeters (4 ft) long with an outside diameter of 2.03 centimeters (0.8 in.). The uranium dioxide fuel is deposited on the interior walls of the pin cladding with a void space running axially for most of the length of the pin. The pin is operated such that the interior fuel surface is at a temperature of 2600° C. Vapor phase mass transport within the central void maintains a constant temperature over the internal fuel surface independent of external variations in neutron flux or heat transfer to the coolant.

The major conclusions of this study are

1. The vapor transport fuel pin can operate at a higher power density than a conventional pin. This effect is particularly noticeable at the larger pin diameters. Since a major percentage of reactor cost is in fuel pin fabrication this effect alone could result in a significant economic benefit. Other factors that affect power reactor costs are beyond the scope of this report.

2. Under certain conditions a vapor transport fuel pin can be operated above the critical heat flux without the clad material reaching thermal failure temperatures. This suggests that superheated steam could be produced from a properly designed single-stage reactor.

3. The startup rate for a vapor transport pin would be determined by the time required for vapor transport to occur without burning out the pin. This startup time could be reduced by making the initial fuel distribution approximately the same as that for the final steady-state operating condition.

Lewis Research Center,
National Aeronautics and Space Administration,
Cleveland, Ohio, November 16, 1970,
122-28.

APPENDIX A

BOILING HEAT TRANSFER CORRELATIONS USED IN THE FUEL PIN CALCULATIONS

Case 1: Heat Transfer Calculations for the Fuel Pin Startup Code

The calculated fuel pin surface temperature (eq. (10)) is used to obtain a surface heat flux from a heat flux as a function of temperature driving force curve for boiling water.

The curve is divided into the four regions which are described in the following sections (ref. 3). Figure 8 illustrates the relation of the four regions to each other.

Region 1. - This is the forced-convection regime where

$$q_o^{(1)} = h_1 (T_s - T_4) \tag{A1}$$

The forced-convection heat-transfer coefficient h_1 is given by

$$h_1 = 0.023 \left(\frac{k_4}{d_{eq}}\right)\left(\frac{d_{eq} v \rho}{\mu}\right)^{0.8}\left(\frac{C_p \mu}{k_4}\right)^{0.4}\left(\frac{R_a}{R_o}\right)^{0.45} \tag{A2}$$

where the physical properties are those of the bulk coolant stream (ref. 4).

Region 2. - Region 2 is the partial nucleate boiling regime where

$$q_o^{(2)} = q_o^{(1)}\left[1 + \left\{\frac{q_o^{(3)}}{q_o^{(1)}}\left(1 - \frac{q_i}{q_o^{(3)}}\right)\right\}^2\right]^{1/2} \tag{A3}$$

This is an interpolation formula for the boiling curve in the transition region between forced convection heat transfer and fully developed nucleate boiling.

The term q_i is the fully developed nucleate boiling heat flux at the surface-coolant temperature difference at which local boiling first occurs. It can be obtained graphically as shown in figure 5-4 of reference 3.

The onset of local boiling is given by the intersection of the forced convection curve (eq. (A1)) and the expression for local boiling heat flux q_{LB} where

$$q_{LB} = 1.1 \times 10^{-4} P_c^{1.156} \left[1.8 (T_s - T_{sat})\right]^{\left[2.3/(14.7 P_c)^{0.0234}\right]} \tag{A4}$$

Note that equation (A4) requires that pressure be in atmospheres and temperature be in ^{o}C to give a heat flux q_{LB} in kilowatts per square centimeter.

Region 3. - This is the fully developed nucleate boiling regime where

$$q_o^{(3)} = (14.7P_c)^{4/3}\left[1.8\,(T_s - T_{sat})\right]^3 \times 6.4\times10^{-10} \tag{A5}$$

Equation (A5) requires that pressure be in atmospheres and that temperature be in ^{o}C to give $q_o^{(3)}$ in Btu/(hr)(ft^2) kilowatts per square centimeter.

Region 4. - Region 4 is the film boiling regime where

$$q_o^{(4)} = h_4\,(T_s - T_4) + \epsilon\sigma\,(T_s^4 - T_{sat}^4) \tag{A6}$$

Note that absolute temperature (K) must be used in equation (A6).

The heat-transfer coefficient h_4 is calculated from

$$h_4 = 0.005\left(\frac{k_{4_s}}{d_{eq}}\right)\left(\frac{d_{eq}V\rho_s}{\mu_s}\right)\left(\frac{C_{p_s}\mu_s}{k_{4_s}}\right)^{0.5} \tag{A7}$$

All physical properties in equation (A7) are determined at the temperature of the pin surface.

Between regions 3 and 4 there is another transition region between fully developed nucleate boiling and film boiling. Since information is not reliable for the region, it was omitted in the code. The transition to film boiling is treated as a discontinuity in the boiling curve which results in conservative calculation of surface temperature.

The critical heat flux q_{crit} determines the point at which fully developed nucleate boiling changes to film boiling. For the purposes of this study a critical heat flux relation was fabricated from available data to give values representative of experimental data in the range of interest. The relation is

$$q_{crit} = 11.3\left(\frac{V_{(1)}}{305}\right)^{1/2}\left(\frac{P_c}{68.1}\right)^{1/4}(1 - \chi)^{1/2} \tag{A8}$$

Equation (A8) is for use in this study only and should not be used as a design equation.

In this study transition to film boiling also occurs if the steam fraction of coolant, on a volume basis, exceeds 0.80.

Case 2: Fully Redistributed Fuel Code Heat-Transfer Calculation

The heat flux as a function of temperature driving force curve is constructed as in case 1 using equations (A1) to (A8). In case 2, however, a surface temperature is obtained from a known value of the surface heat flux.

APPENDIX B

TEMPERATURE DEPENDENT THERMAL CONDUCTIVITY CORRELATIONS

In the calculations presented in this report the thermal conductivity is allowed to vary with temperature in the axial direction. This appendix includes the correlation used to obtain thermal conductivities for the uranium dioxide fuel, the stainless-steel clad, and the coolant water as a function of these temperatures.

UO_2 Fuel. - Except for the first axial increment, the temperature used is the arithmetic mean of the inside clad temperature and the inside fuel temperature of the $(J-1)^{th}$ increment (J^{th} increment for $J=1$). The thermal conductivity correlations are (ref. 5)

$$k_2 = -13.86\times10^{-6}\,\overline{T}_2 + 21.284\times10^{-3} \qquad \overline{T}_2 \le 667\ K \tag{B1}$$

$$k_2 = -3.56\times10^{-6}\,\overline{T}_2 + 11.442\times10^{-4} \qquad 667\ K < \overline{T}_2 < 1220\ K \tag{B2}$$

$$k_2 = 6.1702\times10^{-3} \qquad \overline{T}_2 \ge 1220\ K \tag{B3}$$

The average fuel temperatures are all in K. The units on k_2 are (cal)(cm)/(sec)(cm^2)(^oC).

Stainless-steel 347 clad. - Except for the first axial increment, the temperature used is the arithmetic mean of the inside and outside clad temperature for the $(J-1)^{th}$ increment (J^{th} increment for $J=1$). The thermal conductivity of the clad is (ref. 6)

$$k_3 = 6.75\times10^{-5}\,\overline{T}_3 + 33.25\times10^{-3} \tag{B4}$$

The units on k_s are cal/(sec)(cm^2)(^oC/cm) for $\overline{T}_3$ given in K.

Coolant water. - The temperature of the coolant is considered to be $T_{4(J)}$ in ^oC. The thermal conductivity of the coolant water is (ref. 7)

$$k_4 = 8.15\times10^{-7}\,T_4 + 1.515\times10^{-3} \qquad T_4 \le 150^o\ C \tag{B5}$$

$$k_4 = -1.164\times10^{-6}\,T_4 + 1.805\times10^{-3} \qquad 150^o\ C < T_4 < 250^o\ C \tag{B6}$$

$$k_4 = 4.76\times10^{-6}\,T_4 + 2.702\times10^{-3} \qquad 250^o\ C \le T_4 \le T_{sat} \tag{B7}$$

$$k_4 = 1.63\times10^{-4} \qquad T_4 > T_{sat} \tag{B8}$$

The units on k_4 are (cal)(cm)/(sec)(cm^2)(^oC).

REFERENCES

1. Rom, Frank E.; Finnegan, Patrick M.; and McDonald, Glen E.: Very-High-Burnup Vapor-Transport Fuel-Pin Concept for Long-Life Nuclear Reactors. NASA TN D-4860, 1968.

2. McLain, Stuart; and Martens, J. H., eds.: Reactor Handbook. Vol. 4. Second ed., Interscience Publ., 1964.

3. Tong, L. S.: Boiling Heat Transfer and Two-Phase Flow. John Wiley & Sons, Inc., 1965.

4. Bennett, C. O.; and Myers, J. E.: Momentum, Heat, and Mass Transfer. McGraw-Hill Book Co., Inc., 1962, p. 340.

5. Tipton, C. R., Jr., ed.: Materials. Vol. 1 of Reactor Handbook. Second ed., Interscience Publ., 1960.

6. Weiss, V.; and Sessler, J. G., eds.: Aerospace Structural Metals Handbook. Vol. I: Ferrous Alloys. Syracuse University Press, Mar. 1963.

7. Weast, R. C.; Selby, S. M.; and Hodgman, C. D., eds.: Handbook of Chemistry and Physics. 46th ed., Chemical Rubber Co., 1965.

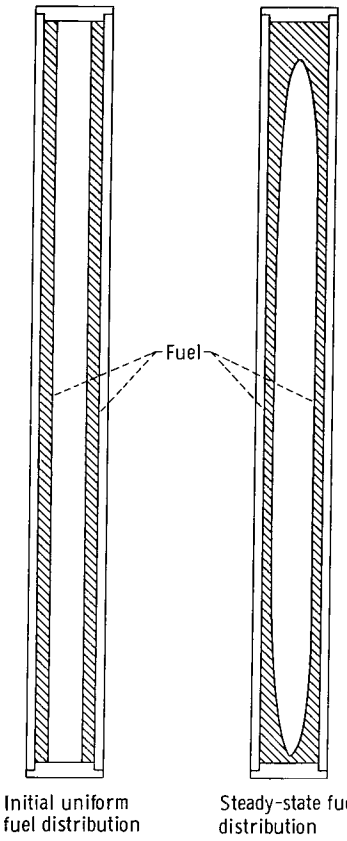

Figure 1. - Fuel distribution before irradiation and after the fuel has been fully redistributed. Data are that of the reference case.

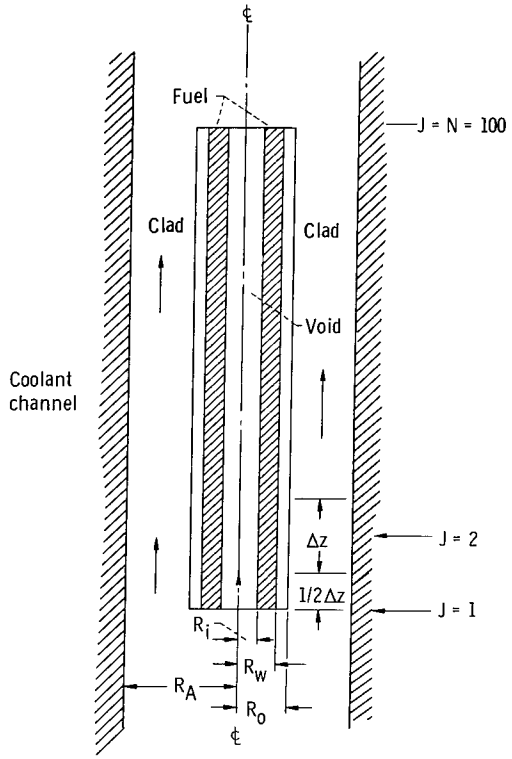

Figure 2. - Schematic diagram of fuel pin model used in mathematical analysis.

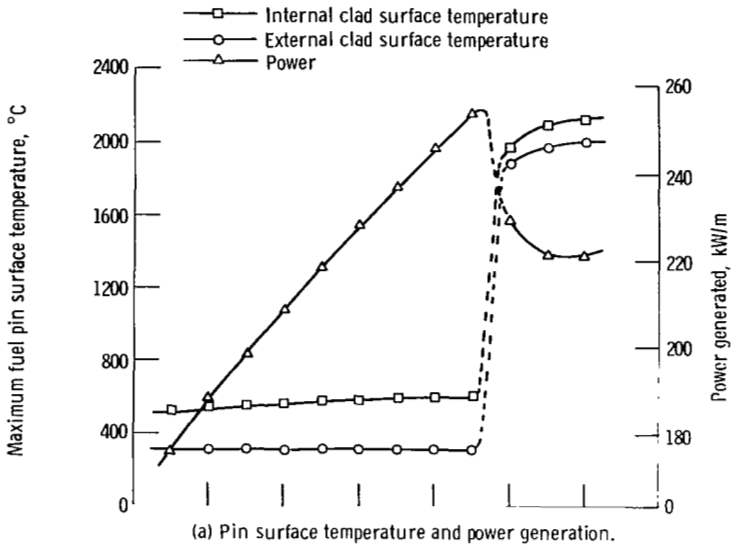

(a) Pin surface temperature and power generation.

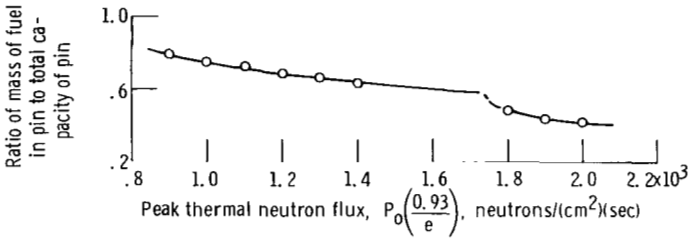

(b) Fuel void fraction.

Figure 3. - Effect of neutron flux level.

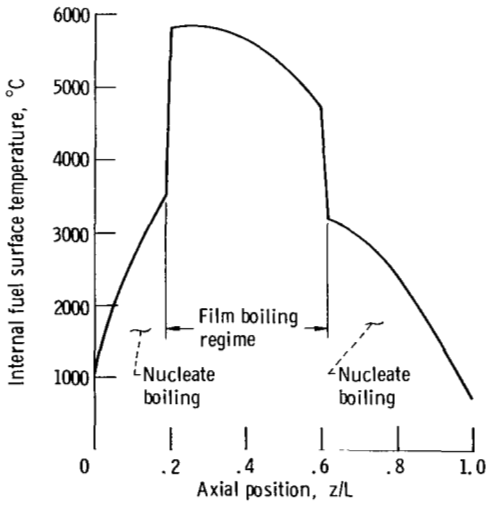

Figure 4. - Initial fuel pin temperature distribution at startup for conditions of reference case. Fuel is uniformly distributed.

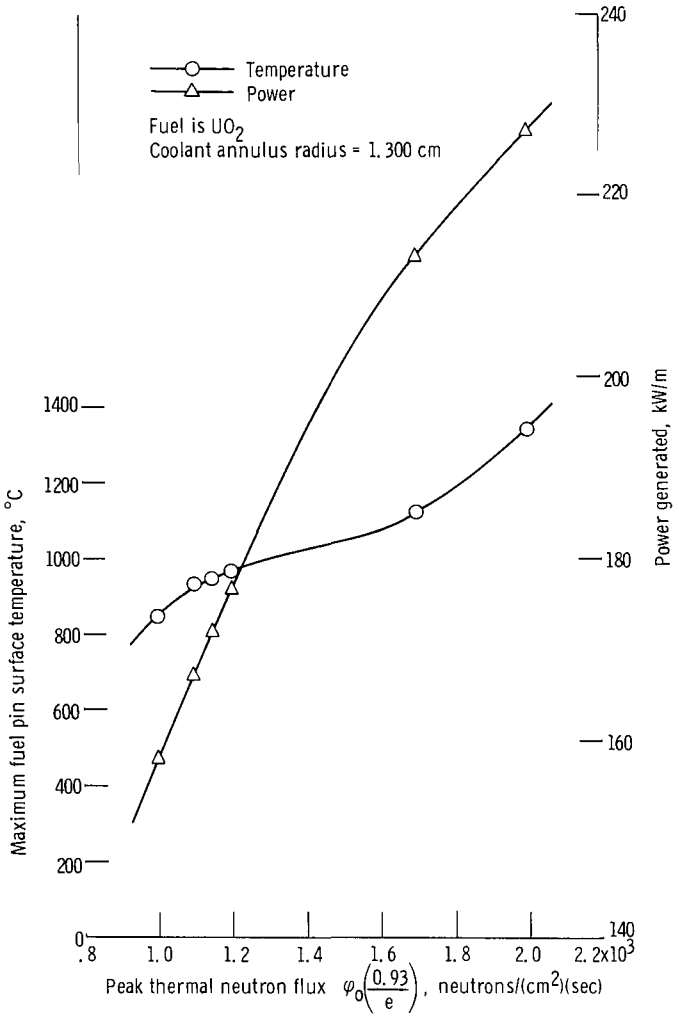

Figure 5. - Maximum surface temperature and total power output as functions of unperturbed thermal neutron flux. Fuel, uranium dioxide; coolant annulus radius, 1.300 centimeters. (The coolant annulus radius is 0.302 centimeter less than that of the reference case.

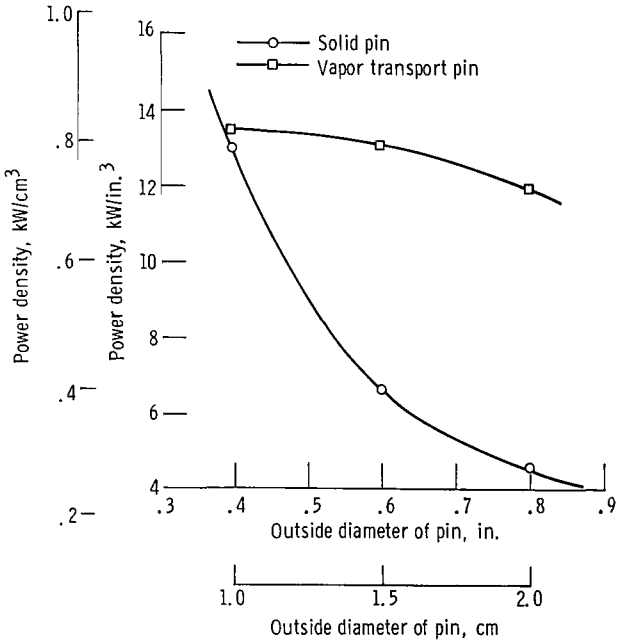

Figure 6. - Comparison of vapor transport pin with conventional fuel element. Critical heat flux is not exceeded for either pin. Clad thickness, 1 inch.

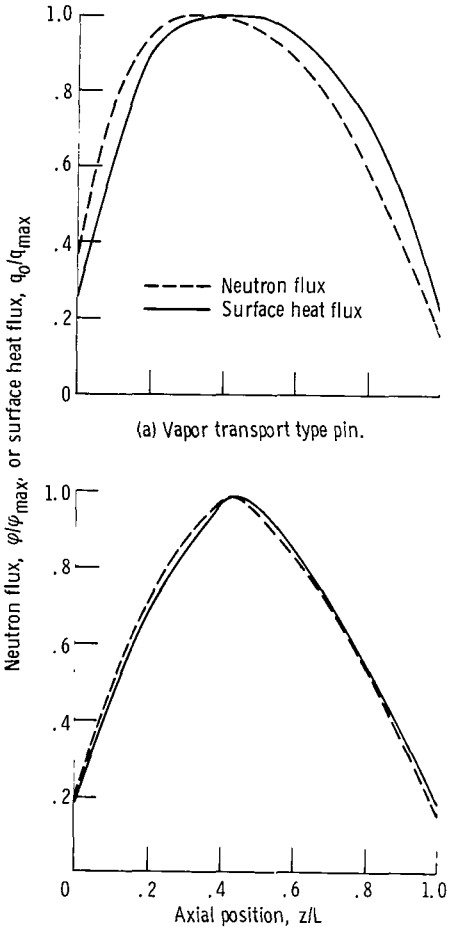

(a) Vapor transport type pin.

(b) Conventional solid fuel pin.

Figure 7. - Neutron flux at fuel surface and surface heat flux distributions for both vapor transport and conventional solid fuel pins. Pin diameter, 0.8 inch (2.030 cm); reference case conditions.

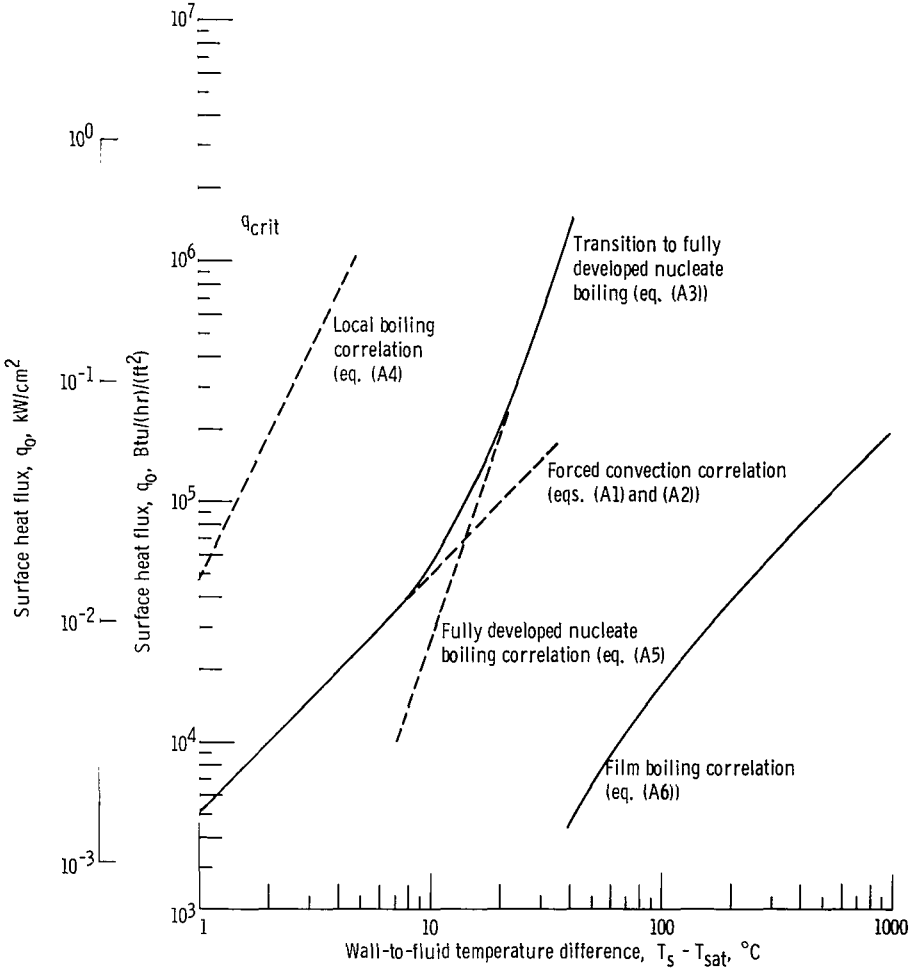

Figure 8. - Boiling heat transfer curves for conditions at coolant inlet end of reference pin.

"The aeronautical and space activities of the United States shall be conducted so as to contribute . . . to the expansion of human knowledge of phenomena in the atmosphere and space. The Administration shall provide for the widest practicable and appropriate dissemination of information concerning its activities and the results thereof."

—NATIONAL AERONAUTICS AND SPACE ACT OF 1958

NASA SCIENTIFIC AND TECHNICAL PUBLICATIONS

TECHNICAL REPORTS: Scientific and technical information considered important, complete, and a lasting contribution to existing knowledge.

TECHNICAL NOTES: Information less broad in scope but nevertheless of importance as a contribution to existing knowledge.

TECHNICAL MEMORANDUMS: Information receiving limited distribution because of preliminary data, security classification, or other reasons.

CONTRACTOR REPORTS: Scientific and technical information generated under a NASA contract or grant and considered an important contribution to existing knowledge.

TECHNICAL TRANSLATIONS: Information published in a foreign language considered to merit NASA distribution in English.

SPECIAL PUBLICATIONS: Information derived from or of value to NASA activities. Publications include conference proceedings, monographs, data compilations, handbooks, sourcebooks, and special bibliographies.

TECHNOLOGY UTILIZATION PUBLICATIONS: Information on technology used by NASA that may be of particular interest in commercial and other non-aerospace applications. Publications include Tech Briefs, Technology Utilization Reports and Technology Surveys.

Details on the availability of these publications may be obtained from:

SCIENTIFIC AND TECHNICAL INFORMATION OFFICE

NATIONAL AERONAUTICS AND SPACE ADMINISTRATION

Washington, D.C. 20546